LOGIC
Journal of Engineering Design and Technology
Vol. 26 No.1 March 2026 ; p. 29 - 38

p-ISSN : 1412-114X
e-ISSN : 2580-5649
http://ojs2.pnb.ac.id/index.php/LOGIC

MATHEMATICAL MODELING AND THERMAL ANALYSIS OF A THERMOELECTRIC COOLER BOX USING A WATER-COOLING BLOCK AND HEATSINK–FAN SYSTEM

I Nyoman Agus Adi Saputra[1)], Adi Winarta[1)*], I Wayan Sutina[1)]

1) Department of Mechanical Engineering, Politeknik Negeri Bali Jl. Kampus Bukit Jimbaran, Badung, Bali 80362

Corresponding email [1)*] : adi.winarta@pnb.ac.id

Abstract. This study presents a mathematical modeling and thermal performance analysis of a Thermoelectric Cooler Box equipped with two hot-side heat rejection systems: a Water Cooling Block and a Heatsink–Fan. Thermoelectric cooling offers an environmentally friendly alternative to vapor-compression refrigeration because it operates without refrigerants and requires only low-voltage DC power. The objective of this work is to evaluate the influence of electrical current on temperature distribution, cooling capacity (Q_c), and the coefficient of performance (COP) of a TEC1-12706 module under both cooling configurations. The mathematical model is formulated based on the energy balance between the cold and hot sides, incorporating the Peltier effect, thermal conduction, and Joule heating losses. Numerical simulations were performed in Python for currents ranging from 1 to 7 A. The results show that the WCB reduces the hot-side temperature (T_h) by 6–8 °C compared with the HSF, indicating superior heat rejection. However, despite producing a lower T_c and larger ΔT, the WCB yields slightly lower Q_c (<10%) and COP (≈5–7%) because lower T_c reduces the $\alpha I T_c$ term and larger ΔT increases back-conduction. The maximum COP for both systems occurs at 3-4 A, corresponding to a temperature difference (ΔT) of approximately 28 °C. Although the cooling capacity of the WCB is slightly lower (<10%) due to increased back-conduction, it offers better thermal stability and long-term performance consistency. Overall, the developed mathematical model captures the TEC's thermal behavior and is supported by comparison with published TEC1-12706 performance trends, providing a reliable foundation for optimizing water-cooled thermoelectric designs. This work contributes an explicit WCB–HSF comparison across operating current to highlight performance tradeoffs for cooler-box design.

Keywords : Thermoelectric Cooler (TEC), Water Cooling Block (WCB), Heatsink–Fan, Coefficient of Performance (COP), Mathematical Modeling

1. INTRODUCTION

The demand for efficient, compact, and environmentally friendly cooling systems continues to increase alongside advancements in modern technology. Conventional vapor-compression cooling systems generally offer high efficiency; however, their use presents several issues, including high energy consumption, the use of refrigerants that may harm the ozone layer, and limited flexibility for small-scale applications [1]. Consequently, there is growing interest in alternative cooling technologies that are simpler and more environmentally sustainable. These concerns are widely summarized in review studies [2], [3].

One promising solution is the Thermoelectric Cooler (TEC), which utilizes the Peltier effect to generate cooling without the need for working fluids. When an electric current is applied, TEC modules absorb heat from one side

(cold side) and release it on the opposite side (hot side). These characteristics make TECs widely used in portable cooling systems, food and medicine storage, medical devices, and electronic component cooling such as computer processors. The main advantages of TEC systems include their simple structure, absence of vibration, refrigerant-free operation, and ease of electronic control [4].

However, TEC-based cooling systems have an inherent drawback in the form of low thermal efficiency. This low efficiency is primarily caused by limitations in heat dissipation on the hot side of the module. If the heat from the hot side is not effectively removed, the module temperature will rise, reducing the temperature differential between the hot and cold sides and consequently decreasing cooling capacity [5]. In addition, increasing the electrical current supplied to the module generates Joule heating losses, which further degrade cooling performance [6].

To address these issues, a more effective heat dissipation system is required. One widely adopted innovation is the integration of a Water Cooling Block (WCB) and a heatsink–fan (HSF) assembly on the hot side of the thermoelectric module. This combination enables faster heat removal because the water inside the WCB has a high heat capacity and can absorb thermal energy efficiently [7], [8]. Meanwhile, the heatsink–fan accelerates air convection, allowing the heat absorbed by the coolant to be released rapidly into the environment. This integrated system has been proven to reduce the hot-side temperature and directly improve cooling performance and the Coefficient of Performance (COP). However, systematic and design-oriented comparisons of WCB versus compact HSF under identical TEC modules, boundary conditions, and operating-current sweeps particularly for cooler-box configurations remain limited, leaving the performance tradeoffs insufficiently quantified.

Several previous studies have demonstrated that water-based cooling significantly enhances TEC system efficiency [9], [10]. Research by Adeniji et al. reported that the use of a water cooling block could reduce hot-side temperature by more than 15 °C compared with natural air cooling [11]. Similarly, Sharma found that increasing the water flow rate in a WCB system improved cooling capacity by up to 25% before reaching thermal saturation [12]. These findings emphasize that effective heat dissipation design is a key factor in improving thermoelectric performance [13].

Although various experimental studies have been conducted, purely experimental approaches have limitations in explaining the complex interactions between electrical and thermal aspects within the system [14]. Therefore, a mathematical modeling approach is needed to describe system behavior comprehensively. Such an approach enables analysis of the relationships among electrical current, temperature difference, heat transfer rate, and COP without requiring repetitive physical testing. Mathematical models can also be used to determine optimal operating conditions and evaluate the effectiveness of additional heat dissipation components such as WCBs and heatsink–fans in improving overall system efficiency. Lumped-parameter, energy-balance TEC models are commonly used to predict T_c, T_h, Q_c, and COP and to identify optimum operating current, providing a justified basis for the present approach [15], [16].

This study specifically focuses on the mathematical modeling and thermal performance analysis of a Thermoelectric Cooler Box (TECB) equipped with a Water Cooling Block (WCB) and a heatsink–fan. Unlike prior work that often evaluates a single heat-rejection option or reports limited operating points, this study applies a unified model and Python-based current sweep to directly compare WCB and HSF for the TEC1-12706 under consistent assumptions, thereby making the performance tradeoffs (temperature distribution, Q_c, and COP) explicit for cooler-box design. The novelty of this research lies in combining mathematical modeling with Python-based numerical simulations to compare the efficiency of two heat dissipation systems (WCB and HSF) for the TEC1-12706 module, a topic that has received limited attention in previous literature [8], [17].

2. METHODS

The cooling system modeled in this study consists of a single thermoelectric (TEC) module installed between a cold plate and a hot-side heat rejection system (either a Water Cooling Block (WCB) or a heatsink–fan (HSF), depending on the configuration analyzed). On the hot side, heat generated by the module is transferred to the coolant water through conduction in the WCB (WCB configuration) or directly to the surrounding air through the heatsink–fan (HSF configuration). Meanwhile, the cold side of the module absorbs heat from the air inside the cooler box through a lumped/effective internal convection coefficient h_{box} [2], [3].The cooling process is driven by the Peltier effect, whereas the primary heat losses originate from Joule heating due to the applied electrical current and back-conduction of heat from the hot side to the cold side [15], [16]. The schematic design of the system, including the heat flow direction and the function of each component, is shown in Figure 1.

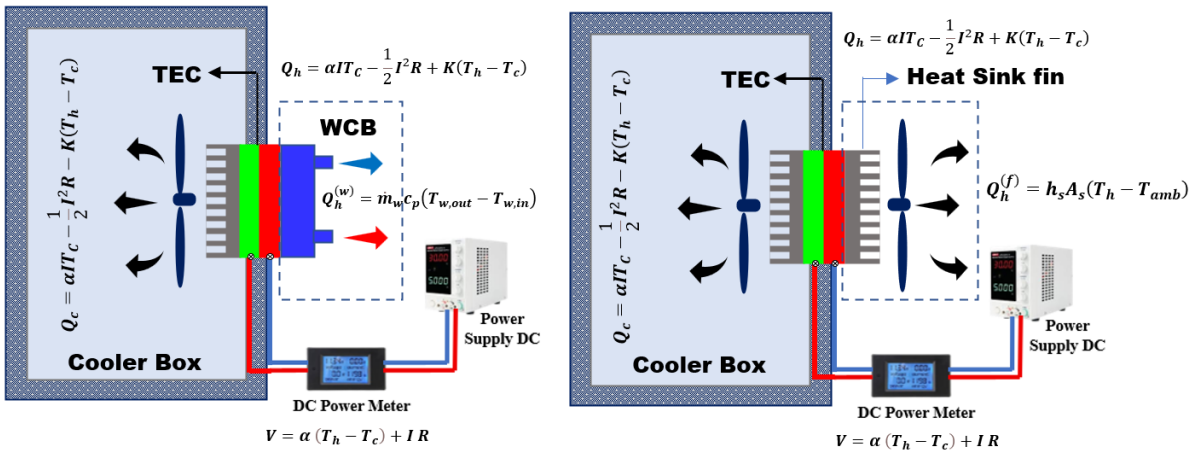

Figure 1. Schematic of the mathematical model of the Thermoelectric Cooler Box (TEC) equipped with a Water Cooling Block (WCB) and a heatsink–fan.

To simplify the calculation process, the present model adopts several assumptions. The thermoelectric (TEC) module material is considered homogeneous and isotropic. Heat transfer is assumed to occur only in one dimension, from the cold side to the hot side. The ambient temperature is maintained at 30 °C. Heat transfer through the WCB and heatsink is treated as a steady-state process, and the cooling effect due to natural convection is neglected on the hot-side external heat rejection path in comparison with forced convection generated by the fan. In contrast, heat transfer on the cold side is represented using the effective internal coefficient h_{box} (Table 1) to couple the box air to the cold surface. For each operating current, T_c and T_h are solved as steady-state values (quasi-steady current sweep), and transient cooling of the box air is not considered in this model.
The operating current in the simulation ranges from 1 A to 7 A, with increments of 1 A. For each current level, the cold-side temperature (T_c), hot-side temperature (T_h), absorbed heat load (Q_c), rejected heat (Q_h), and the coefficient of performance (COP) are calculated based on the ratio between cooling capacity and electrical input power.
The mathematical modeling of the Thermoelectric Cooler Box (TEC–WCB–Heatsink–Fan) system is derived from the energy balance on both the cold and hot sides of the thermoelectric module. The model incorporates the three dominant mechanisms governing TEC operation: the Peltier effect, thermal conduction, and Joule heating resulting from the applied electrical current [10], [18]. All thermal/electrical parameters and symbols used in the governing relations are defined with units in the corresponding parameter tables.

Table 1. Input data for the mathematical simulation of the TEC–WCB–Heatsink system.

No	Parameter	Symbol	Value	Unit	Description
1	Seebeck coefficient	α	0.045	V/K	Voltage generated per temperature difference across the TEC module
2	Internal electrical resistance	R_mod	2.5	Ω	Internal electrical resistance of the TEC module
3	Thermal conductivity of TEC module	K_th	0.5	W/K	Heat conduction between the hot and cold sides of the TEC
4	Ambient temperature	T_amb	30.0	°C	Temperature of the surrounding air
5	Initial temperature inside the box	T_box	25.0	°C	Initial air temperature inside the cooling chamber
6	Convective heat transfer coefficient (cold side)	h_box	5.0	W/m²K	Convective heat transfer coefficient on the cold side
7	Cold-side surface area	A_c	0.02	m²	Contact area between TEC cold side and cooler box
8	Heatsink convective coefficient	h_s	50.0	W/m²K	Convective heat transfer coefficient on the hot side
9	Heatsink surface area	A_s	0.03	m²	Heat transfer area on the hot side
10	Contact area of water block	A_wb	0.01	m²	Heat transfer area between water cooling block and TEC

11	Water mass flow rate	ṁ_w	0.15	kg/s	Mass flow rate of coolant in the water block
12	Water density	ρ_w	1000.0	kg/m³	Density of coolant (water)
13	Dynamic viscosity of water	μ_w	1×10^{-3}	Pa·s	Dynamic viscosity of water at room temperature
14	Specific heat capacity of water	c_p	4182.0	J/kg·K	Heat capacity of water
15	Thermal conductivity of water	k_w	0.6	W/m·K	Thermal conductivity of water
16	Hydraulic diameter of coolant channel	D_h	0.01	m	Hydraulic diameter of the water block channel
17	Operating current range	I	1.0 – 7.0	A	Current range used in TEC performance simulation

The mathematical modeling of the Thermoelectric Cooler system (TEC–WCB–Heatsink–Fan) is developed based on the energy balance between the cold and hot sides of the TEC module. The relationship between the electrical and thermal parameters of the TEC is expressed through a series of equations (1–21), as presented in Tables 2 and 3. To avoid ambiguity, each equation is accompanied by explicit variable definitions; Eq. (20) is provided as an algebraic rearrangement of Eq. (2) for computational convenience, hence they are identical in form and outcome.

Table 2. Basic mathematical formulations for the Thermoelectric Cooler (TEC) module

Limitations	Calculations	No
Cold-side temperature	$T_c = T_h - \Delta T_0 + \beta I$	(1)
Hot-side temperature	$T_h = T_{amb} + Q_h R_{th,total}$	(2)
Temperature difference between the hot and cold sides	$\Delta T = T_h - T_c$	(3)
Cooling capacity at the cold side	$Q_c = \alpha I T_c - \frac{1}{2} I^2 R - K(T_h - T_c)$	(4)
Heat rejection rate at the hot side	$Q_h = \alpha I T_c - \frac{1}{2} I^2 R + K(T_h - T_c)$	(5)
Electrical voltage across the TEC module	$V = \alpha(T_h - T_c) + IR$	(6)
Total electrical power input	$P_t = VI = \alpha I(T_h - T_c) + I^2 R$	(7)
Coefficient of Performance (COP)	$COP = \frac{Q_c}{P_t}$	(8)
Optimum operating current	$I_{opt} = \frac{K(T_h - T_c)}{\alpha(T_h - T_c) + \frac{1}{2}R}$	(9)

Table 3. Heat transfer parameters of the Water Cooling Block (WCB)

Limitations	Calculations	No
Cooling water mass flow rate	$\dot{m}_w = \rho_w A_{ch} V_w$	(10)
Heat dissipated by the Water Cooling Block	$Q_h^{(w)} = \dot{m}_w c_{p,w}(T_{w,out} - T_{w,in})$	(11)
Heat dissipated by the heatsink–fan assembly	$Q_h^{(f)} = h_s A_s (T_h - T_{amb})$	(12)
Reynolds number of the cooling water flow	$Re = \frac{\rho_w u D_h}{\mu_w}$	(13)

Prandtl number of the coolant	$Pr = \frac{c_{p,w}\mu_w}{k_w}$	(14)
Nusselt number (Dittus–Boelter correlation)	$Nu = 0.023\, Re^{0.8} Pr^{0.4}$	(15)
Convective heat transfer coefficient of the WCB	$h_w = \frac{Nu\, k_w}{D_h}$	(16)
Convective thermal resistance of the WCB	$R_{th,w} = \frac{1}{h_w A_w}$	(17)
Convective thermal resistance of the heatsink–fan	$R_{th,hs} = \frac{1}{h_s A_s}$	(18)
Total thermal resistance on the hot side	$R_{th,total} = R_{th,TEC} + R_{th,w} + R_{th,hs}$	(19)
Hot-side temperature based on total thermal resistance	$T_h = T_{amb} + Q_h R_{th,total}$	(20)
Cold-side temperature derived from the box air temperature	$T_c = T_{box} + Q_c R_{th,cold}$	(21)

The mathematical formulations (1)–(21) described above constitute the foundation of the numerical model used to predict the temperature distribution, cooling capacity, and coefficient of performance of the Thermoelectric Cooler Box (TEC) system under two cooling configurations: the Water Cooling Block (WCB) and the heatsink–fan (HSF). All equations were implemented using Python programming, with operating current variations ranging from 1 to 7 A to obtain the thermal performance profile of the system. Each current point is treated as a steady-state operating condition (quasi-steady sweep), and transient responses are outside the present scope.

3. RESULTS AND DISCUSSION

3.1 Cold-Side Temperature Response Under Varying Electrical Current

Figure 2 illustrates the relationship between electrical current and the cold-side temperature (T_c) for the two cooling configurations, namely the Water Cooling Block (WCB) and the heatsink fan (HSF). The graph shows that increasing the current results in a decrease in cold-side temperature for both systems. However, the temperature reduction in the WCB configuration is significantly greater than in the HSF system [10], [11]. This phenomenon occurs because, in thermoelectric systems, higher current intensifies the Peltier effect, which governs heat transfer from the cold side to the hot side of the TEC module. As the current increases, more electrons transport thermal energy, resulting in stronger cooling on the cold side. Nevertheless, this beneficial effect is only maintained if the heat on the hot side (T_h) can be effectively dissipated to the environment. In the HSF configuration, heat rejection relies solely on forced-air convection, where air has relatively low specific heat capacity (C_p) and thermal conductivity compared with water. In contrast, the WCB system utilizes water as the coolant, enabling faster heat absorption through conduction and forced circulation. This mechanism helps maintain a stable and lower hot-side temperature (Th), thereby increasing the temperature difference ($\Delta T = T_h - T_c$). These results confirm that the effectiveness of heat removal on the hot side has a direct impact on cold-side cooling performance. Consequently, the WCB provides superior thermal stability for the TEC module, reduces the risk of overheating, and sustains optimal cooling performance over longer operating durations [19]. However, the larger ΔT produced by WCB also increases conductive heat leakage (back-conduction, $K\Delta T$) from the hot side to the cold side, which can reduce net Qc and COP even when Tc becomes lower (discussed later in Sections 3.2–3.3).

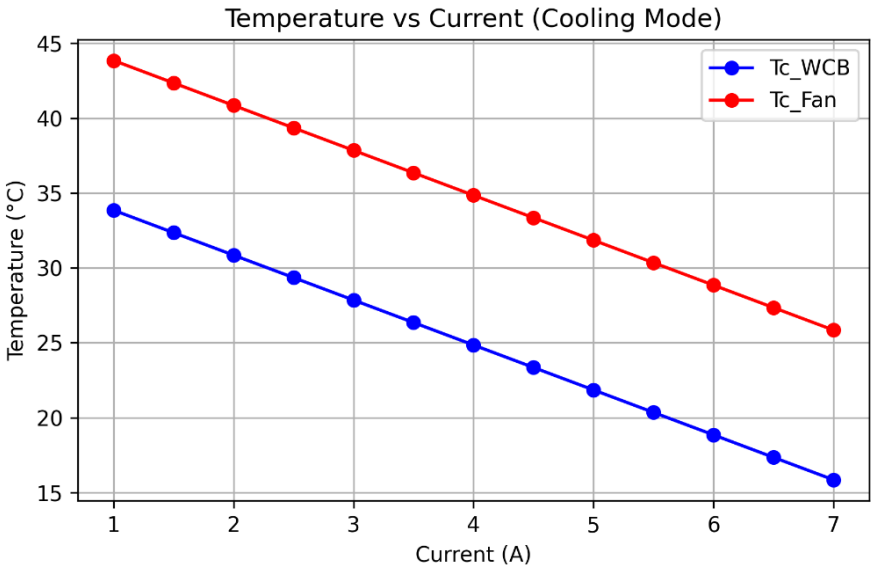

Figure 2. Relationship between electrical current and cold-side temperature ($T_{(c)}$ of WCB and $T_{(c)}$ of HSF).

3.2 Cooling Capacity Characteristics as a Function of Electrical Current

Figure 3 presents the relationship between cooling capacity (Q_c) and electrical current (I). In general, both the WCB and the HSF systems exhibit an increasing trend in Q_c as the current increases. This behavior aligns with the fundamental theory of the Peltier effect, where the cooling capacity is proportional to the applied current up to the optimum operating limit of the module. However, the simulation results show that the Q_c values of the HSF system are slightly higher than those of the WCB system across all current levels.

The relation of cooling capacity and current can be explained using the Peltier equation. At a given current, the net cooling capacity may be written as: $Q_c = \alpha I T_c - \frac{1}{2} I^2 R - K\Delta T$ where $\alpha I T_c$ is the Peltier cooling term, $\frac{1}{2} I^2 R$ is the Joule-heating penalty, and $K\Delta T$ represents back-conduction. The WCB system produces a lower cold-side temperature (T_c) due to its more effective hot-side heat dissipation. A lower T_c reduces the contribution of the $\alpha I T_c$ term in the Peltier cooling equation, resulting in a slightly lower Q_c compared with the HSF system [20], [21]. Nevertheless, the difference is relatively small (<10%) and does not indicate a substantial reduction in performance. Another factor influencing this behavior is back-conduction ($K\Delta T$). Since the WCB system maintains a larger temperature difference ΔT, conductive heat losses between the cold and hot sides become slightly higher, which further decreases the net Q_c [22], [23]. From a practical standpoint, these findings indicate that although the HSF system yields slightly higher cooling output, it does so at the cost of higher hot-side temperature and reduced thermal stability; moreover, achieving the same low T_c as WCB would typically require higher current and thus higher electrical power input. In contrast, the WCB system offers superior thermal stability and overall efficiency, even though its Q_c values are marginally lower.

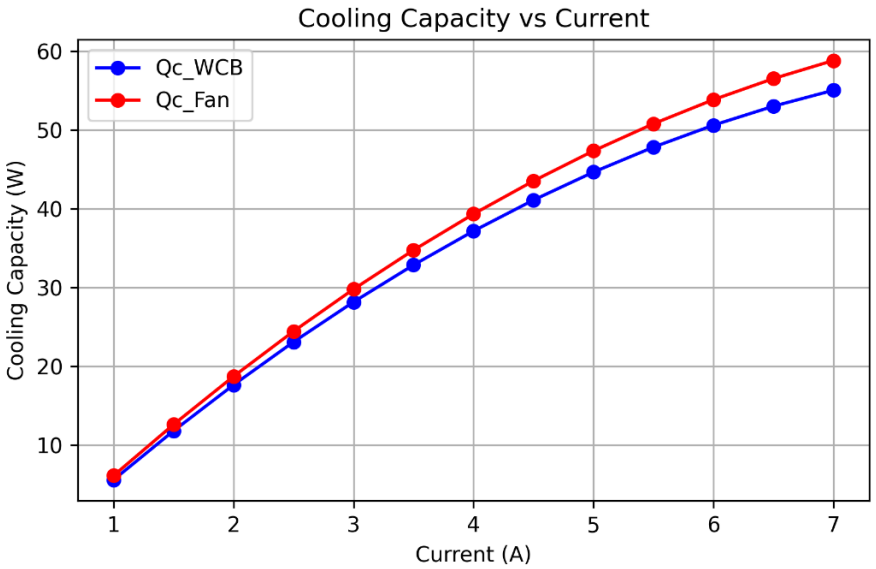

Figure 3. Variation of cooling capacity (Q_c) for WCB and HSF systems with electrical current.

3.3 Coefficient of Performance Trend with Increasing Electrical Current

Figure 4 shows the relationship between the Coefficient of Performance (COP) and the electrical current. Both systems exhibit similar characteristics: the COP increases at low currents, reaches a peak at approximately I = 3–4 A, and then decreases at higher currents. This behavior reflects the existence of an optimal operating point for the thermoelectric module. At low currents, an increase in current causes Qc to rise more rapidly than the electrical power input (Pt = V × I), leading to improved efficiency. However, at higher currents, power losses due to Joule heating (I^2R) become dominant, resulting in a reduction in COP [10]. Across the entire current range, the HSF system consistently achieves slightly higher COP values compared with the WCB system. This behavior is associated with the lower cold-side temperature (T_c) produced by the WCB configuration, which reduces the $\alpha I T_c$ term in the Peltier cooling equation, leading to a slightly lower net cooling capacity under the same operating current [20], [21]. In other words, although WCB increases ΔT and lowers T_c, the net Q_c can decrease because the $\alpha I T_c$ term drops while the back-conduction loss $K\Delta T$ increases; since $COP = Q_c/P_{in}$ and P_{in} is comparable at the same current, this slightly lower Q_c translates into a slightly lower COP. Even so, the performance difference remains small (approximately 5–7%), indicating that both systems operate within similar efficiency ranges. Despite having a slightly lower COP, the WCB configuration maintains superior thermal stability due to more effective heat rejection at the hot side. By keeping Th lower and more stable, WCB minimizes thermal accumulation and preserves a stronger temperature gradient across the TEC module, which contributes to long-term reliability and reduces thermal degradation [22], [23]. The maximum COP of the WCB system reaches approximately 0.78, while the HSF system peaks at around 0.83 within the 3–4 A range. These findings are consistent with previous studies reporting that water-based heat exchangers enhance hot-side heat removal, improve thermal uniformity, and optimize operational conditions for thermoelectric devices [24]. Liu et al. further demonstrated that COP is strongly dependent on hot-side fluid temperature, aligning with the present results that show improved performance stability in systems using water cooling [25]. This emphasizes the critical importance of efficient heat rejection in maximizing the performance of thermoelectric cooling systems [26]. Overall, the simulation results demonstrate that the TEC system equipped with a Water Cooling Block and a heatsink–fan provides a more balanced heat distribution between the hot and cold sides. The stable ΔT observed in the medium current range (approximately 2–4 A), along with the maximum COP occurring within this interval, indicates that the system can operate efficiently when the current is adjusted to its optimal value. These findings agree with earlier studies highlighting that enhanced hot-side cooling significantly improves thermoelectric efficiency [19], [27]. Therefore, the mathematical model developed in this study successfully represents the physical behavior of the TEC and can serve as a foundation for design optimization using CFD simulations or for future experimental validation. In real implementation, WCB is generally more suitable for long-duration operation, higher ambient temperatures, or applications prioritizing thermal stability and reliability (at the expense of added components such as pump/tubing), whereas HSF is more suitable for low-cost, compact, and portable systems where simplicity and ease of maintenance are primary requirements.

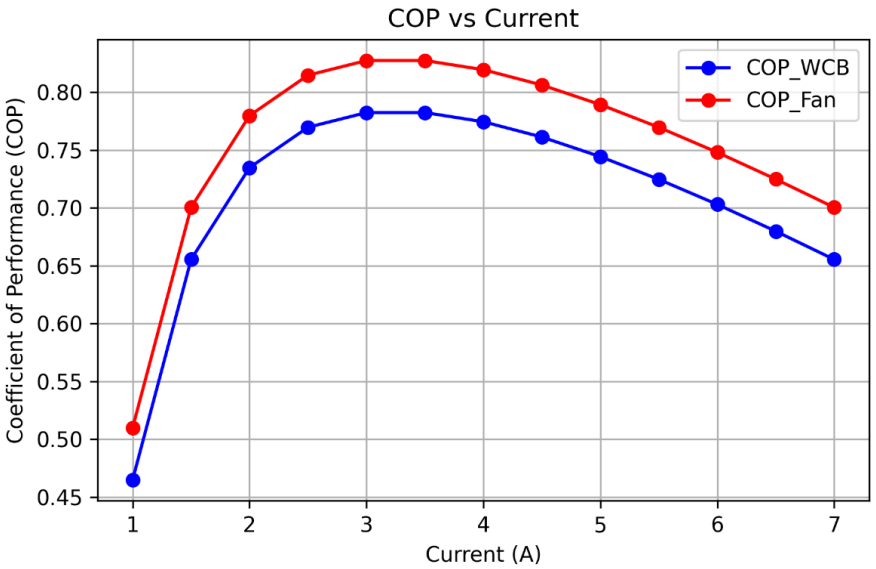

Figure 4. Comparison of COP between the WCB and HSF systems.

4. CONCLUSION

Based on the results of the mathematical modeling and numerical analysis conducted in this study, the following conclusions can be drawn:

1. Increasing the electrical current supplied to the thermoelectric module (TEC1-12706) leads to a rise in the hot-side temperature (T_h) and a decrease in the cold-side temperature (T_C), reaching an optimum point at approximately 4 A, where the maximum temperature difference (ΔT) is about 28 °C.
2. The Water Cooling Block (WCB) configuration is capable of maintaining a lower hot-side temperature, achieving 6–8 °C lower T_h compared with the Heatsink–Fan (HSF) system. This confirms that the water-cooling approach provides more effective heat rejection than air-based cooling.
3. The cooling capacity (Qc) of the WCB system is slightly lower (<10%) than that of the HSF system due to increased back-conduction heat transfer resulting from the larger ΔT. Nevertheless, the WCB system demonstrates superior thermal stability, especially during sustained operation.
4. The maximum COP for both systems occurs at medium current levels (≈3–4 A), which represents the most efficient operating point before Joule heating (I^2R) becomes dominant.
5. Simulation results indicate that the HSF system achieves a slightly higher COP (about 5–7%) than the WCB system over the entire current range. However, the WCB configuration still provides better long-term stability, as its more effective hot-side cooling reduces thermal accumulation and maintains a stronger temperature gradient across the TEC module.
6. The mathematical model developed in this study successfully captures the physical behavior of the TEC system, including the interaction of Peltier cooling, Joule heating, back conduction, and hot-side heat removal. Therefore, it can serve as a foundation for design optimization, CFD-based investigations, or future experimental validation of water-cooled thermoelectric systems. From a design perspective, these results imply that selecting WCB versus HSF should be based on the target application: WCB is preferable when hot-side temperature control and long-duration stability are critical, while HSF is preferable when simplicity, compactness, and lower system complexity are prioritized, with the operating current ideally maintained near 3–4 A for efficient performance.

5. REFERENCES

[1] M. Mirmanto, S. Syahrul, M. Wirawan, I. M. A. Sayoga, A. T. Wijayanta, and I. Mahyudin, "Performance of a Thermoelectric Powered by Solar Panel for a Large Cooler Box," *Adv. sci. technol. eng. syst. j.*, vol. 5, no. 1, pp. 325–333, Feb. 2020, doi: 10.25046/aj050141.

[2] K. Zhu *et al.*, "A general White–Box strategy for designing thermoelectric cooling system," *InfoMat*, vol. 4, no. 11, p. e12324, Nov. 2022, doi: 10.1002/inf2.12324.

[3] Z. Xu, C. Li, H. Zhao, Y. Zheng, and J. Zhang, "Design and performance analysis of hot side heat sink of thermoelectric cooler device based on simulation and experiment," *Energy Science & Engineering*, vol. 11, no. 12, pp. 4463–4480, Dec. 2023, doi: 10.1002/ese3.1591.

[4] F. A. M. A. Ali, S. M. A. M. Reda, M. A. M. Hussein, S. K. Ayed, L. Jassim, and H. S. Majdi, "Thermoelectric-Driven Room Air Cooling via a Multi-U Shaped Heat Sink System," *IJHT*, vol. 41, no. 4, pp. 1000–1006, Aug. 2023, doi: 10.18280/ijht.410421.
[5] E. Yudiyanto, R. S. Setiabudi, A. Hardjito, S. Adiwidodo, and B. Pranoto, "Effect of Velocity and Type of Cooling Fluid on Peltier Heat Transfer for Car Cabin Cooling Applications," *JSAE*, vol. 5, no. 2, p. 76, Sep. 2022, doi: 10.31328/jsae.v5i2.4036.
[6] P. E. Ruiz-Ortega, M. A. Olivares-Robles, and C. A. Badillo-Ruiz, "Transient thermal behavior of a segmented thermoelectric cooler with variable cross-sectional areas," *Int J Energy Res*, vol. 45, no. 13, pp. 19215–19225, Oct. 2021, doi: 10.1002/er.7123.
[7] B. Pfeiffelmann, A. C. Benim, and F. Joos, "Water-Cooled Thermoelectric Generators for Improved Net Output Power: A Review," *Energies*, vol. 14, no. 24, p. 8329, Dec. 2021, doi: 10.3390/en14248329.
[8] N. T. Atmoko, A. Jamaldi, and T. W. B. Riyadi, "An Experimental Study of the TEG Performance using Cooling Systems of Waterblock and Heatsink-Fan," *AE*, vol. 5, no. 3, pp. 261–267, Jun. 2022, doi: 10.31603/ae.6250.
[9] Kennedy, K. Anwar, A. Muis, B. Basri, and M. Ilhamsyah, "Effect of thermoelectric placement on the commercial waterblock to the liquid cooling system performance," *J. Phys.: Conf. Ser.*, vol. 1763, no. 1, p. 012039, Jan. 2021, doi: 10.1088/1742-6596/1763/1/012039.
[10] Politeknik Negeri Bali, I. W. Sutina, A. Winarta, Politeknik Negeri Bali, I. N. A. A. Saputra, and Politeknik Negeri Bali, "Performance Analysis of Thermoelectric Cooler Box with Water Cooling Block (WCB) and Heat Sink Fan," *LOGIC*, vol. 25, no. 2, pp. 93–99, Jul. 2025, doi: 10.31940/logic.v25i2.93-99.
[11] A. P. Adeniji, R. Sule, E. I. Ogunwale, and W. A. Ayara, "Development and Performance Evaluation of Portable water-cooling system using thermoelectric peltier modules," *IOP Conf. Ser.: Earth Environ. Sci.*, vol. 1492, no. 1, p. 012024, Apr. 2025, doi: 10.1088/1755-1315/1492/1/012024.
[12] H. Sharma, G. Saxena, R. Randa, and R. S. Rajput, "Novel hybrid vehicle battery cooling system: Integrating Peltier-based heat sinks for control of thermal management," *Proceedings of the Institution of Mechanical Engineers, Part C: Journal of Mechanical Engineering Science*, vol. 239, no. 17, pp. 7135–7157, Sep. 2025, doi: 10.1177/09544062251343501.
[13] N. Numan, M. Mahdi, and M. Ahmed, "A Comparative Experimental Study Analysis of Solar Based Thermoelectric Refrigerator Using Different Hot Side Heat Sink," *ETJ*, vol. 40, no. 1, pp. 90–98, Jan. 2022, doi: 10.30684/etj.v40i1.2058.
[14] B. I. Robertson, Y.-H. Shin, and J.-W. Choi, "A Thermoelectric Temperature Control Module for a Portable Fluorescent Sensing Platform," *J. Electrochem. Soc.*, vol. 167, no. 14, p. 147505, Nov. 2020, doi: 10.1149/1945-7111/abc35d.
[15] E. Fang, X. Wu, Y. Yu, and J. Xiu, "Numerical modeling of the thermoelectric cooler with a complementary equation for heat circulation in air gaps," *Open Physics*, vol. 15, no. 1, pp. 27–34, Mar. 2017, doi: 10.1515/phys-2017-0004.
[16] L. Li *et al.*, "Performance Optimization of a Thermoelectric-Water Hybrid Cooling Garment," *Adv Materials Technologies*, vol. 9, no. 21, p. 2301069, Nov. 2024, doi: 10.1002/admt.202301069.
[17] Y. Ma, M. Zhao, J. Li, J. Wang, and L. Hu, "Cooling Effect of Different Land Cover Types: A Case Study in Xi'an and Xianyang, China," *Sustainability*, vol. 13, no. 3, p. 1099, Jan. 2021, doi: 10.3390/su13031099.
[18] T. N. Widianto and C. Mahendra, "Kinerja Susunan dan Jumlah Elemen Peltier pada TEC Alat Transportasi Ikan Segar," *JPBKP*, vol. 14, no. 1, p. 75, Jun. 2019, doi: 10.15578/jpbkp.v14i1.567.
[19] M. J. Dousti and M. Pedram, "Platform-dependent, leakage-aware control of the driving current of embedded thermoelectric coolers," in *International Symposium on Low Power Electronics and Design (ISLPED)*, Beijing, China: IEEE, Sep. 2013, pp. 311–316. doi: 10.1109/ISLPED.2013.6629315.
[20] Z. Tark, A. J. Hamed, and A. H. N. Khalifa, "Performance Study of the Thermoelectric Personal Cooler under Different Ambient Temperatures," *IJHT*, vol. 40, no. 1, pp. 53–62, Feb. 2022, doi: 10.18280/ijht.400107.
[21] T. Tanehira, Y. Furubayashi, A. Yamamoto, K. Yonemori, S. Miyoshi, and S.-I. Kuroki, "Calculation of Seebeck Coefficients for Advanced Heat Transfer Modules," *ECS Trans.*, vol. 80, no. 5, pp. 57–62, Aug. 2017, doi: 10.1149/08005.0057ecst.
[22] N. Wang *et al.*, "An Enhanced Thermoelectric Collaborative Cooling System With Thermoelectric Generator Serving as a Supplementary Power Source," *IEEE Trans. Electron Devices*, vol. 68, no. 4, pp. 1847–1854, Apr. 2021, doi: 10.1109/TED.2021.3059183.
[23] P. Kolber, D. Perczyński, and K. Peszyński, "Investigation of A Thermoelectric Cooling System Based on A Peltier Module Using A Temperature Chamber," presented at the Engineering Mechanics 2020, 2020, pp. 278–281. doi: 10.21495/5896-3-278.
[24] A. Żelazna and J. Gołębiowska, "A PV-Powered TE Cooling System with Heat Recovery: Energy Balance and Environmental Impact Indicators," *Energies*, vol. 13, no. 7, p. 1701, Apr. 2020, doi: 10.3390/en13071701.

[25] Z. B. Liu, L. Zhang, G. Gong, Y. Luo, and F. Meng, "Experimental study and performance analysis of a solar thermoelectric air conditioner with hot water supply," *Energy and Buildings*, vol. 86, pp. 619–625, Jan. 2015, doi: 10.1016/j.enbuild.2014.10.053.
[26] K. Roungbungrud, P. Chantawong, and J. Khedari, "Development of a Stand-Alone Thermoelectric Power Generator Using Heat of Refrigerant Leaving the Condenser and Self-Cooled by Condensate of a Split-Type Air Conditioning," *IJHT*, vol. 40, no. 3, pp. 737–742, Jun. 2022, doi: 10.18280/ijht.400311.
[27] S. B. Riffat and G. Q. Qiu, "Design and characterization of a cylindrical, water-cooled heat sink for thermoelectric air-conditioners," *Int. J. Energy Res.*, vol. 30, no. 2, pp. 67–80, Feb. 2006, doi: 10.1002/er.1124.